IEEE Access
Multidisciplinary | Rapid Review | Open Access Journal

Received May 13, 2019, accepted May 31, 2019, date of publication June 5, 2019, date of current version June 19, 2019.

Digital Object Identifier 10.1109/ACCESS.2019.2921108

Transformer Incipient Hybrid Fault Diagnosis Based on Solar-Powered RFID Sensor and Optimized DBN Approach

TAO WANG[1], YIGANG HE[2], (Member, IEEE), TIANCHENG SHI[1], AND BING LI[1]
[1]School of Electrical Engineering and Automation, Hefei University of Technology, Hefei 230009, China
[2]School of Electrical Engineering, Wuhan University, Wuhan 430072, China

Corresponding author: Yigang He (18655136887@163.com)

This work was supported in part by the National Natural Science Foundation of China under Grant 51577046, in part by the State Key Program of National Natural Science Foundation of China under Grant 51637004, in part by the National Key Research and Development Plan "Important Scientific Instruments and Equipment Development" under Grant 2016YFF0102200, and in part by the Equipment Research Project in Advance under Grant 41402040301.

ABSTRACT This paper introduces a novel hybrid fault diagnosis method for power transformer. This method employs solar-powered radio-frequency identification (RFID) sensor for transformer vibration signal acquisition and deep belief network (DBN) for feature extraction. The customized RFID sensor employs solar panel as a power source, and a supercapacitor is adopted to be the stand-by power when the solar panel cannot work. A charging circuit is exploited to guarantee constant DC output voltage. The collected hybrid faults signal is characterized as nonlinear and nonstationary; moreover, it contains abundant noises and harmonic components, which makes it difficult to acquire succinct and robust features from the raw signals. Hence, the DBN is adopted to extract features from the collected vibration signal. In order to obtain optimum feature extraction performance, the quantum particle swarm optimization algorithm (QPSO) is employed to determine the hidden layer structure and learning rate of the DBN model. The experiments indicate that the proposed RFID sensor is able to realize reliable data acquisition and transmission. Besides, the optimized DBN achieves remarkable results in feature extraction for the hybrid fault signal and achieves high diagnosis accuracy.

INDEX TERMS Transformer, incipient fault diagnosis, solar-powered RFID sensor, deep belief network.

I. INTRODUCTION

The operation state of power transformer is closely related to the reliable operation of the power grid. During the operation time of transformer, the short circuit current and electro-magnetic force would cause damage to the transfer, and the mechanical failure is the most serious type [1]–[3]. The mechanical failures are mainly resulted from the winding or core, and it is hard to be recognized in its early stage, so the mechanical failure would always cause great economic loss [4], [5]. Therefore, it is essential to find the transformer's mechanical failure in early stage.

Several transformer fault diagnosis approaches have already been proposed. The dissolved gas analysis (DGA) and low voltage impulse test (LVI) are able to distinguish the faults' type, but the fault's location cannot be determined [6], [7]. Frequency response analysis (FRA) [8] has high diagnosis accuracy, but the low voltage winding needs to be disconnected during the measurement process. Short circuit reactance (SCR) [9] is capable of realizing live-line measurement, so the transformer can keep operating during the measurement procedure. But the failure's location and category cannot be obtained [12]. Recently, Ultra-Wide Band (UWB) technique is proposed in the field of transformer fault diagnosis, and both the location and type of failure can be obtained [13], [14]. For the time being, this approach can only detect the condition of winding. Moreover, this method needs UWB transceivers and Vivaldi antenna for measurement, it would increase the diagnosis cost. Vibration analysis has drawn great attention in the field of mechanical fault diagnosis since it is easy to be realized and characterized as live line measurement [15]–[21]. In our previous study [22]–[24], we have employed RFID sensor and the vibration analysis approach to realize non-intrusive fault

The associate editor coordinating the review of this manuscript and approving it for publication was Vincenzo Piuri.

diagnosis and prognosis of transformer with low costs and high accuracy. In [23] the stacked denoising autoencoder is employed for transformer fault diagnosis and has shown satisfactory performance, it focuses on the diagnosis of single fault, when several types of fault happen simultaneously, they cannot achieve satisfactory result. Moreover, all these methods perform fault diagnosis after the fault happens, so the transformer has already been damaged and caused the economic loss. Therefore, this paper aims to realize the fault diagnosis when the failure is in the incubation period, which is the incipient fault diagnosis. In this period, the failure shows no influence on the transformer operation, but the failure may deteriorate rapidly in the following time, resulting in the shutdown of transformer. In this way, the transformer can be fixed before serious failure happens, and the economic loss can be significantly reduced.

In the field of mechanical fault diagnosis, a lot of signal processing approaches are employed, such as Wavelet packet transform [25], HHT analysis [26], time-frequency analysis [27], [28], and sparse representation [29], [30]. However, the state-of-art approaches requires deep understanding on the fault signal and prior knowledge about signal processing and mechanical system. With the rapid development of computer science, the deep learning approach has been a hot topic especially in recent years. The deep learning technique tries to train a deep neural network that can realize automatically feature extraction and other tasks [31]–[33].

The deep belief network (DBN) [34]–[36] is an unsupervised deep learning approach which has proven to be effective in terms of feature extraction. DBN can effectively avoid the over-fitting phenomenon to the training data set via unsupervised pre-training. Compared with the traditional unsupervised models, DBN can obtain the laws in the deep layer which hiding in multiple features and achieve better generalization ability. Therefore, this paper employs DBN for feature extraction of transformer hybrid incipient faults. In existing studies, the hidden layer structure and learning rate is set on the basis of experience, but the feature learning performance cannot always be optimum. To solve this problem, the quantum behaved particle swarm optimization algorithm (QPSO) is employed to find the optimum hidden layer structure and learning rate.

The frequency spectrum is employed as the input data for feature extraction and has achieved diagnosis accuracy over 97% [37], [38]. Therefore, in this paper, the frequency spectrum obtained by EEMD is used as the input of DBN.

This work aims to introduce a hybrid fault diagnosis method for transformer mechanical failure in early stage with advantages of high accuracy, low cost and high stability. Compared with previous research, this paper realizes the diagnosis for transformer incipient hybrid fault. To realize optimum diagnosis performance, the hidden layer structure and learning rate of DBN is optimized by using QPSO algorithm, besides, the envelop spectrum of raw signal is selected as the input data to further improve the diagnosis performance. The solar-powered RFID sensor design is shown in Section II. Section III describes the theories of fault diagnosis. Section IV discusses the experiments detail and results. The conclusion drawn from the study is shown in Section V.

II. SOLAR-POWERED RFID SENSOR

Fig. 1 is the solar powered RFID sensor that employed for vibration signal acquisition, it has the same structure with that of in [24]. The low dropout voltage regulator (TPS780180300DRVR) is adopted to stabilize the output voltage of solar panel and supercapacitor. In this design strategy, the MSP430FR5964 MCU is used for signal processing, it has fast written speed which can write 64kB data within 4ms, and its power consumption is 118 μA/MHz in active mode. The vibration signal is collected by ADXL372 accelerometer sensor which current consumption is 22 μA under 2.5V voltage when measuring. The RFID chip is a typical Monza X-8K, which memory could be accessed by the I^2C interface and UHF interface.

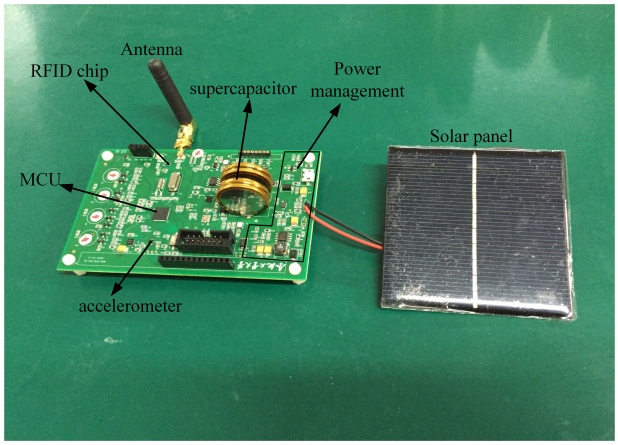

FIGURE 1. Proposed RFID sensor.

As described in [23], a Faraday cage which inner side is made of epoxy resin is employed to reduce the electromagnetic interference to the sensor. Meanwhile, it can also prevent the RFID sensor being damaged by induction voltage. Since the RFID sensor employed in this paper utilizes solar energy as power source, so the solar panel should be outside of the Faraday cage, Fig. 2 shows the packaged RFID sensor.

FIGURE 2. Packaged solar-powered RFID sensor.

III. THEORY

A. RESTRICTED BOLTZMANN MACHINE

The DBN model is constructed by Restricted Boltzman Machine (RBM) via a greedy layer-wise training principle [34]. The RBM model consists of two layers including a visible layer $\boldsymbol{v}=\{0, 1\}^D$ and a hidden layer $\boldsymbol{h}=\{0, 1\}^K$, the architecture of RBM is shown in Fig. 3. Both the visible layer and the hidden layer contains a series of units, and the input data are fed into the visible layer. The energy configuration of the layers is defined as:

$$E(\boldsymbol{v}, \boldsymbol{h}) = -\sum_{p=1}^{D}\sum_{q=1}^{K} v_p w_{pq} h_q - \sum_{p=1}^{D} c_p v_p - \sum_{q=1}^{K} b_q h_q \tag{1}$$

where w_{pq} is the weight between the visible unit p and hidden unit q; c_p and b_q are the bias term of visible unit p and hidden unit q, respectively.

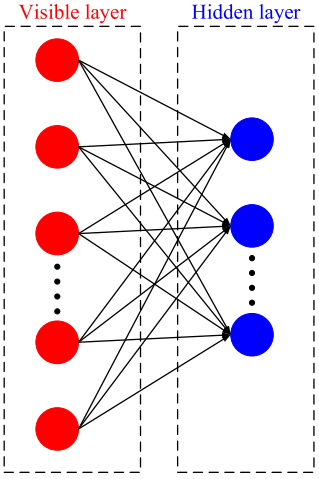

FIGURE 3. Structure of RBM.

The joint distribution of the layers is defined as:

$$t(\boldsymbol{v}, \boldsymbol{h}) = \frac{1}{Z}\exp(-E(\boldsymbol{v}, \boldsymbol{h})) \tag{2}$$

where Z is the normalization constant. From the equation, it can be seen that the probability could be increased by decreasing the energy.

The conditional distribution of visible layer $\boldsymbol{v}$ and hidden layer $\boldsymbol{h}$ can be calculated by the following equations:

$$t(h_q = 1 \,|\boldsymbol{v}) = \sigma(\sum_{p} w_{pq} v_p + b_q) \tag{3}$$

$$t(v_p = 1 \,|\boldsymbol{h}) = \sigma(\sum_{q} w_{pq} h_q + c_p) \tag{4}$$

$$\sigma(s) = \frac{1}{1+\exp(-s)} \tag{5}$$

The contrastive divergence approach is employed to update the weights, and the weights' variation is calculated by the following equation:

$$\Delta w_{pq} = \varepsilon(v_p h_{qorigin} - v_p h_{qreconstruct}) \tag{6}$$

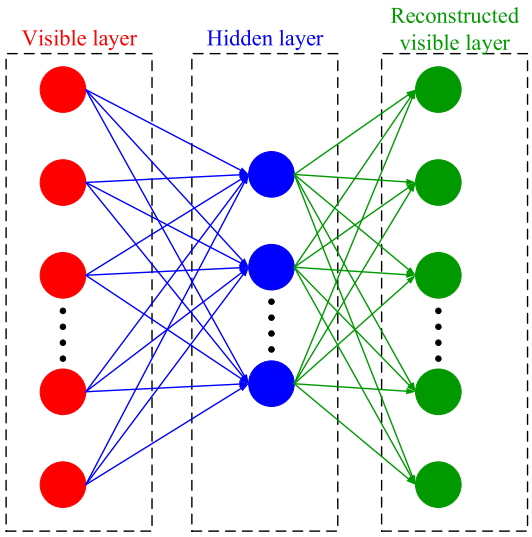

FIGURE 4. Reconstruction procedure of RBM.

where ε is the learning rate. Every RBM model has its own learning rate and the optimum learning rate can generate the suitable weights distribution.

The reconstruction procedure of RBM is shown in Fig. 4. In this procedure, the hidden layer makes attempt to reconstruct a visible layer v1 which can recover the original visible layer v. Then the data obtained in the hidden layer can be thought to be the features of the input data. If the reconstructed data can perfectly recover the original input data, the hidden layer is thought to be effective in terms of learning robust features from the original data.

B. DBN STRUCTURE

Generally, a single stage RBM cannot realize optimum feature learning performance. Thus, several RBMs are stacked to form a deep structure to extract features well. The features extracted by the first RBM are input to the next RBM. Fig. 5 shows the whole training process of a typical DBN with two-stage RBM, the process contains a pre-training and

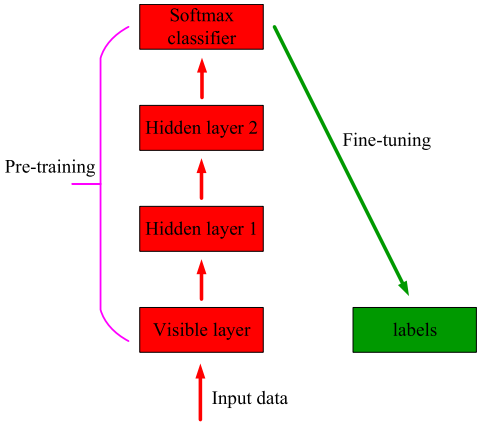

FIGURE 5. The structure of DBN.

a fine-tuning procedure, and the output layer is generally employing the Softmax classifier.

During the pre-training procedure, the input data are processed by the first RBM and the features are learnt, then the learnt features are employed as the input data of the second RBM and the second RBM's features are obtained. This procedure is running in this manner repeatedly, and the features obtained by the last RBM is the extracted features in the pre-training procedure. After that, the features are input into the Softmax classifier layer for fine-tuning.

The pre-trained DBN model is fine-tuned by the Softmax classifier during the fine-tuning process. The Softmax classifier is employed to classify the extracted features in the pre-training process and generate the labels of the features. Then, the generated labels are compared with the input data label and the back-propagation mechanism is employed to minimize the error between these two kinds of labels by updating the weights in the RBM. After the fine-tuning process is finished, the features extracted by the new last RBM is thought to be the learnt features of DBN model.

The learning rate and RBM layers are important parameters to the DBN model, which would significantly influence the feature extraction performance of DBN. Traditionally, these two parameters are selected according to experience, which cannot always find the optimal results. Therefore, in this paper, QPSO is employed to find the optimal values of these two parameters.

C. QPSO

QPSO algorithm introduces the quantum behavior into the convergence mechanism of particle swarm algorithm [39]. Since the quantum behavior characterized as polymorphic and uncertain, it can force the particle can appear at any point in space with some probability and satisfy the requirements of aggregation state in properties difference, so that the particle can search for the global optimal solution more efficiently in the whole space. The particle in QPSO algorithm is iterated as following:

$$mbest = \frac{1}{M}\sum_{i=1}^{M} P_i \tag{7}$$

$$P = \mu P_i + (1-\mu)P_j \tag{8}$$

$$X_i(t+1) = P \pm \alpha\,|mbest - X_i(t)|\ln(1/u) \tag{9}$$

where M is the population size, μ and u are the random numbers with uniform distribution on the interval [0, 1], $mbest$ is the average position of the optimal position of all particles, P_i and P_j is the individual optimal position and global optimal position of i-th particle. $X(t)$ is the position of i-th particle in the t-th iteration, α is the compressive expansion factor. The process of optimizing DBN model by using QPSO can be described as following:

Step 1: initialize QPSO, including the particle position, the searching space, the compressive expansion factor and the iterations, the learning rate and number of hidden layer nodes of DBN is projected as the position of particle;

Step 2: calculate the fitness value of every particle in the group, then calculate the individual optimal position of each particle and the global optimal position of group;

Step 3: calculate the average value of the individual optimal position of all the particles and then update the particles' position;

Step 4: repeat step1to step 3 until meeting the condition of convergence, and the optimization result is the optimal learning rate and number of hidden layer nodes of DBN model.

The employed fitness function during the optimization process is:

$$fit = \frac{1}{RMSE} \tag{10}$$

where $RMSE$ is the root-mean-square error, when the maximum fitness value obtained, the output result is the optimal solution of learning rate. The whole process is illustrated in Fig. 6.

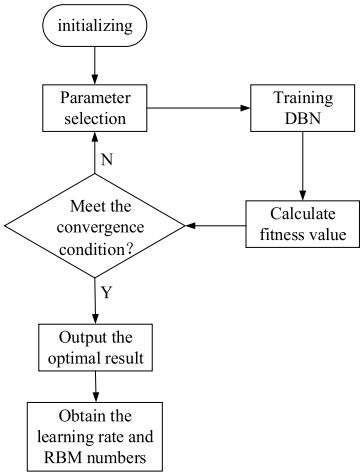

FIGURE 6. The flow chart of optimizing learning rate.

IV. MEASUREMENT RESUTLS

A. EXPERIMENT SETUP

In this experiment, an 110kV three-phase transformer (Fig. 7) is adopted as the test object. The RFID sensor is installed on the shell of transformer for vibration signal acquisition. Table 1 shows the main parameters of the test object.

TABLE 1. Parameters of testing transformer.

Primary voltage (kV)	Secondary voltage (kV)	Rated power (MW)
110	10	50

To evaluate the communication performance of the packaged RFID sensor, the signal-to-noise ratio (SNR) is measured. Fig. 8 shows the measurement results. It can be seen that the packaged sensor shows higher SNR. The RFID

FIGURE 7. Test environment.

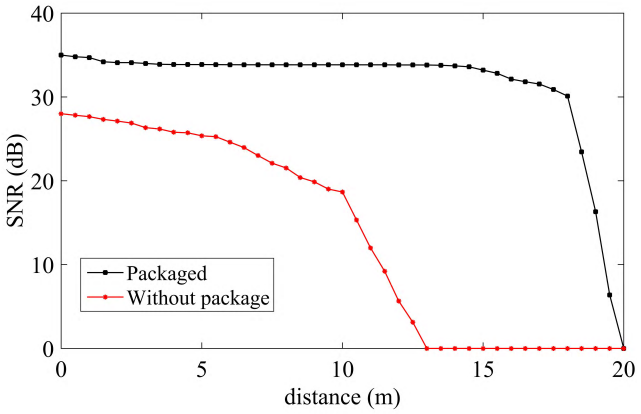

FIGURE 8. SNR measured at different communication distances.

system requires at least 30dB SNR for regular communication [45], thus, from Fig. 8 it can be deduced that the packaged sensor achieves the maximum communication distance of 17.5m.

Ten health conditions of transformer including one normal condition, nine hybrid faults conditions are adopted for diagnosis. The object transformer operates under rated load power. In order to obtain the data of all the hybrid faults conditions, several customized windings and cores are employed (shown in Fig. 9), and each winding or core is artificially damaged to simulate the failure in actual operation.

Table 2 shows the information about these ten conditions, W represents winding, C represents core, D represents deformation, L represents looseness, and O represents overlapping. For each condition under rated load, 1000 signals are collected, it need to be noticed that the frequency spectrum of the vibration signal rather than the signal itself is employed as the input value of DBN. The sample data are normalized before being used for training:

$$x_{norm} = \frac{x - x_{\min}}{x_{\max} - x_{\min}} \tag{11}$$

(a) (b)

FIGURE 9. (a) Customized winding; (b) customized core.

TABLE 2. The health condition of transformer.

Number	Fault Category	Description	Power
F1	Normal	/	Rated
F2	W, W	D, L	Rated
F3	W, W	D, O	Rated
F4	W, W	L, O	Rated
F5	W, C	D, D	Rated
F6	W, C	L, D	Rated
F7	W, C	O, D	Rated
F8	W, W, C	D, L, D	Rated
F9	W. W, C	D, O, D	Rated
F10	W, W, C	L, O, D	Rated

TABLE 3. Optimized hidden layer structure and learning rate.

Algorithm	Hidden layer structure	Learning rate	Training accuracy (%)	Test accuracy (%)	Training time (s)
PSO	500-800-200	0.12	100	89.9	3340
FOA	967-588-835	0.29	100	90.7	3212
QGA	899-631-721	0.47	100	92.8	3473
QPSO	1033-789-847	0.43	100	99.5	3107

where x_{norm} denotes the normalized value, $x_{\min}$ is the minimum value and $x_{\max}$ is and maximum value. Half of the samples are used as training data and the other half as test data.

B. PERFORMANCE OF QPSO

The hidden layer structure and learning rate should be determined before the feature learning process. In order to evaluate the optimization performance of QPSO, particle swarm algorithm (PSO), fruit fly optimization algorithm (FOA) and quantum genetic algorithm (QGA) are also adopted to determine the hidden layers' structure and learning rate. The optimization process of all the optimization process are shown in Fig. 10, the hidden layer structure and learning rate are shown in Table 3. in Fig. 10, the QPSO achieves the best optimization result with minimum fitness value and iterations.

From Table 3 it can be seen that the DBN optimized by QPSO shows highest training accuracy and test accuracy,

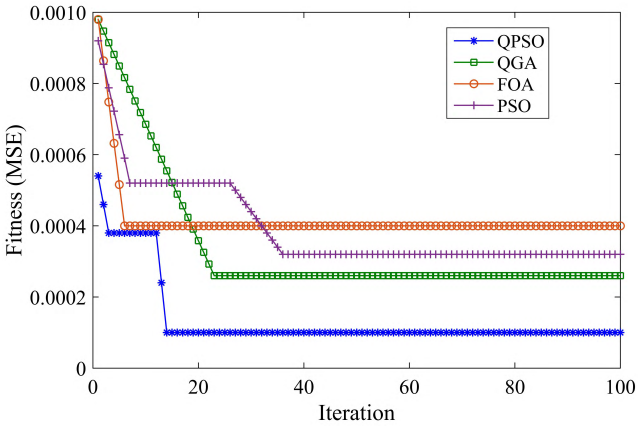

FIGURE 10. The optimization process of different algorithms.

meanwhile, its optimizing time is less than that of PSO and QGA. So, the hidden layer structure of the DBN is 4096-1033-789-847-10, 4096 is the dimension of input data, 10 is the corresponding to the number of transformer condition.

C. PERFORMANCE OF DBN

The performance of DBN in feature learning is compared with that of kernel principal component analysis (KPCA) approach. The test data set contains the ten kinds of conditions listed in Table 2, and the hidden layer structure and learning rate of DBN are determined by using QPSO. Both the two approaches are employed to extract features from the test data set, and the t-SNE (T-Distribution Stochastic Neighbor Embedding) [37] is used to realize the visualization of high dimensional data into a two-dimension feature distribution. The results are shown in Fig. 11, Fig. 11(a) is distribution of raw data, Fig. 11(b) is the feature extracted by KPCA, and Fig. 11(c) is the feature extracted by optimized DBN. When dealing with the hybrid fault conditions, the KPCA method cannot acquire discriminative features, some of the features are mixed. The optimized DBN is able to learn succinct and discriminative features from the hybrid fault signal, which guarantees the fault diagnosis accuracy.

The diagnosis accuracy of the proposed method is compared with the traditional approaches, all the approaches are optimized by QPSO and the results are shown in Table 4. The kernel principal component analysis (KPCA), independent component analysis (ICA) and DBN are employed to extract features from the data, respectively, and the support vector machine (SVM) is employed for classification of the extracted features. It can be seen that under hybrid faults conditions, the proposed DBN achieves the best diagnosis results with highest accuracy and minimal time.

To further evaluate the priority of the introduced Hilbert envelop spectrum in term of fault diagnosis, the raw vibration signal in time domain (F1) and its frequency spectrum (F2) are employed as the input data of SSDA, respectively. The SSDA are optimized by QPSO algorithm, the results are listed in Table 5. For these three kinds of input data, the

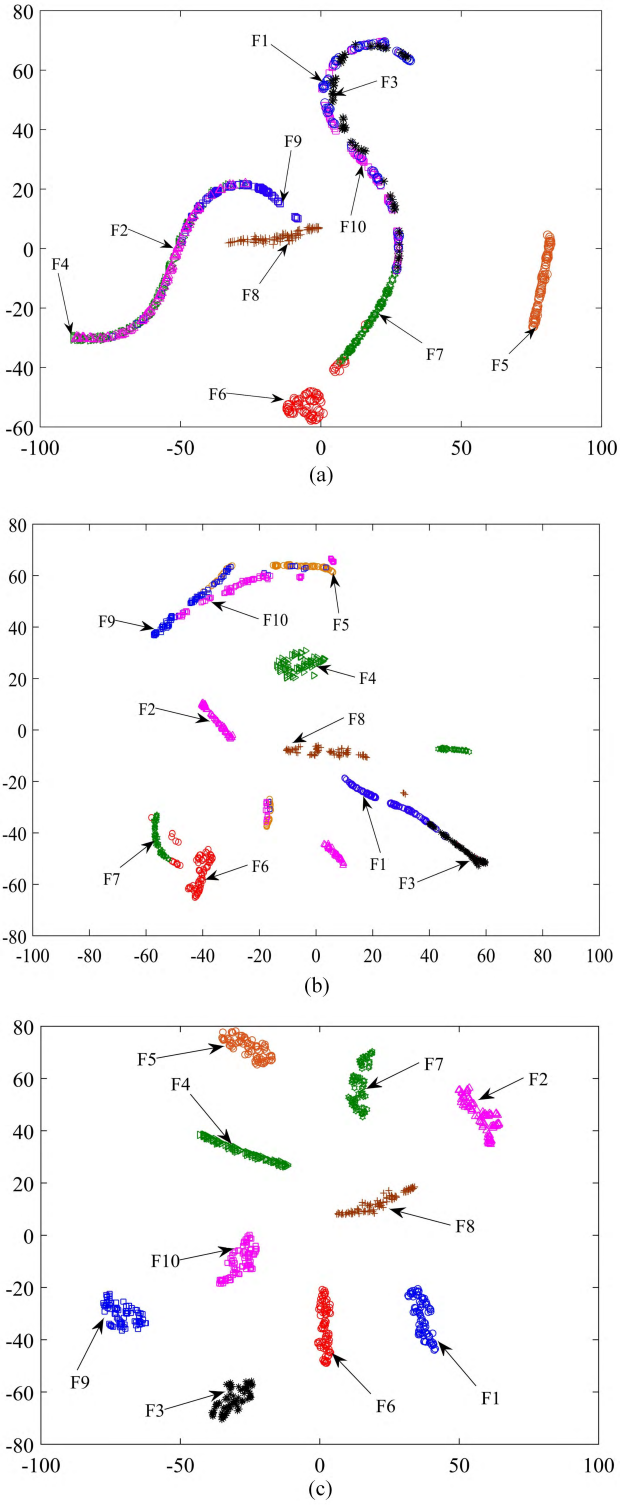

FIGURE 11. Feature extraction performances: (a) raw data; (b) KPCA; (c) DBN.

training accuracy are all 100%, which means the SSDA model has excellent performance in feature learning. But the test accuracy is different for different input data, F1 shows the minimal test accuracy, F2 ranks the second and the introduced

TABLE 4. Fault diagnosis performance comparison.

Approach	Accuracy (%)	Time (s)
KPCA-SVM	65.7	2.258
ICA-SVM	71.1	1.762
This paper	99.8	0.488

TABLE 5. Fault diagnosis performance of Different input feature data.

Input data	Training accuracy (%)	Test accuracy (%)
F1	100	60.5
F2	100	88.1
This paper	100	99.8

input data in this paper achieves the highest test accuracy. This experiment indicates that the feature extracted from F1 cannot represent the whole character of raw signal. As for the frequency spectrum and Hilbert envelop spectrum, the Hilbert envelop spectrum achieves higher test accuracy. Therefore, it can be deduced that the Hilbert envelop spectrum is more sensitive to the fault and has better robustness compared with the other two kinds of input data.

V. CONCLUSION

In this study, a non-invasive, low cost and high accuracy method using solar-powered RFID sensor and DBN is introduced for incipient hybrid fault diagnosis of transformer. The exploited RFID sensor utilizes solar panel to harvest power, a series of supercapacitors are used as stand-by power to improve the sustainability of power supply. During the daytime, the solar panel harvests solar energy to power the RFID sensor and charge the supercapacitors. When the illumination intensity is not adequate for the solar panel to harvest enough power (>2.8V output voltage) for the RFID sensor (such as during the night), the supercapacitor starts to operates as power supply.

The DBN model is aimed to obtain succinct and discriminative features from transformer vibration signals that contains miscellaneous noises and abundant harmonic components. The Hilbert envelop spectrum is employed as the input data of DBN, which promises reliable feature extraction performance as well as fault diagnosis performance. The hidden layer structure and learning rate of DBN is optimized by QPSO approach to guarantee optimal feature extraction results. The experimental results have validated the effectiveness of the proposed approach in learning features from hybrid fault signals, the proposed method can achieve 99.8% fault diagnosis accuracy for the incipient fault.

In the future, the study would focus on the improvement of the RFID sensor and the realization of wireless monitoring system for the whole substation.

REFERENCES

[1] A. E. B. Abu-Elanien, M. M. A. Salama, and M. Ibrahim, "Calculation of a health index for oil-immersed transformers rated under 69 kV using fuzzy logic," *IEEE Trans. Power Del.*, vol. 27, no. 4, pp. 2029–2036, Oct. 2012.

[2] M. Mauntz and J. Peuser, "Continuous condition monitoring of high voltage transformers by direct sensor monitoring of oil aging for a stable power network," in *Proc. IEEE Conf. Diagnostics Elect. Eng. (Diagnostika)*, Sep. 2016, pp. 1–4.

[3] S. Kumar, T. Islam, and K. K. Raina, "Modelling of breather for transformer health assessment," *IET Sci. Meas., Technol.*, vol. 11, no. 2, pp. 194–203, Oct. 2016.

[4] A. Bakshi and S. V. Kulkarni, "Eigenvalue analysis for investigation of tilting of transformer winding conductors under axial short-circuit forces," *IEEE Trans. Power Del.*, vol. 26, no. 4, pp. 2505–2512, Oct. 2011.

[5] T. D. Rybel, A. Singh, J. A. Vandermaar, M. Wang, J. R. Marti, and K. D. Srivastava, "Apparatus for online power transformer winding monitoring using bushing tap injection," *IEEE Trans. Power Del.*, vol. 24, no. 3, pp. 996–1003, Jul. 2009.

[6] S. A. Khan, M. D. Equbal, and T. Islam, "A comprehensive comparative study of DGA based transformer fault diagnosis using fuzzy logic and ANFIS models," *IEEE Trans. Dielectr. Electr. Insul.*, vol. 22, no. 1, pp. 590–596, Feb. 2015.

[7] J. Christian and K. Feser, "Procedures for detecting winding displacements in power transformers by the transfer function method," *IEEE Trans. Power Del.*, vol. 19, no. 1, pp. 214–220, Jan. 2004.

[8] L. Coffeen, J. McBride, N. Woldemariam, and J. Benach, "A summary of NEETRAC on-line frequency response analysis (FRA) a new EPRI commercial prototype FRA installation at first energy," presented at the EPRI Substation Equipment Maintenance Optimiz. Diagnost. Conf., San Antonio, TX, USA, Mar. 2009.

[9] A. Palani, S. Santhi, S. Gopalakrishna, and V. Jayashankar, "Real-time techniques to measure winding displacement in transformers during short-circuit tests," *IEEE Trans. Power Del.*, vol. 23, no. 2, pp. 726–732, Apr. 2008.

[10] P. Gómez, F. de León, and I. A. Hernández, "Impulse-response analysis of toroidal core distribution transformers for dielectric design," *IEEE Trans. Power Del.*, vol. 26, no. 2, pp. 1231–1238, Apr. 2011.

[11] J. Lu, J. Yuan, L. Chen, J. Sheng, and X. Ma, "Calculation of the short-circuit reactance of transformers by a line integral based on surface magnetic charges," *IEEE Trans. Magn.*, vol. 34, no. 5, pp. 3483–3486, Sep. 1998.

[12] H. Rahbarimagham, H. K. Porzani, M. S. A. Hejazi, M. S. Naderi, and G. B. Gharehpetian, "Determination of transformer winding radial deformation using UWB system and hyperboloid method," *IEEE Sensors J.*, vol. 15, no. 8, pp. 4194–4202, Aug. 2015.

[13] S. Mortazavian, M. M. Shabestary, Y. A.-R. I. Mohamed, and G. B. Gharehpetian, "Experimental studies on monitoring and metering of radial deformations on transformer HV winding using image processing and UWB transceivers," *IEEE Trans. Ind. Informat.*, vol. 11, no. 6, pp. 1334–1345, Dec. 2015.

[14] J. Shengchang, Z. Lingyu, and L. Yanming, "Study on transformer tank vibration characteristics in the field and its application," *Przegląd Elektrotechniczny*, vol. 87, no. 2, pp. 205–211, 2011.

[15] J. T. Yoon, B. D. Youn, K. M. Park, and W.-R. Lee, "Vibration-based robust health diagnostics for mechanical failure modes of power transformers," in *Proc. IEEE Conf. Prognostics Health Manage.*, Jun. 2013, pp. 1–5.

[16] S. Borucki, "Diagnosis of technical condition of power transformers based on the analysis of vibroacoustic signals measured in transient operating conditions," *IEEE Trans. Power Del.*, vol. 27, no. 2, pp. 670–676, Apr. 2012.

[17] K. Hong, H. Huang, and J. Zhou, "Winding condition assessment of power transformers based on vibration correlation," *IEEE Trans. Power Del.*, vol. 30, no. 4, pp. 1735–1742, Aug. 2015.

[18] B. Garcia, J. C. Burgos, and A. M. Alonso, "Transformer tank vibration modeling as a method of detecting winding deformations—Part I: Theoretical foundation," *IEEE Trans. Power Del.*, vol. 21, no. 1, pp. 157–163, Jan. 2006.

[19] K. Hong, H. Huang, Y. Fu, and J. Zhou, "A vibration measurement system for health monitoring of power transformers," *Measurement*, vol. 93, pp. 135–147, Nov. 2016.

[20] R. Duan and F. Wang, "Fault diagnosis of on-load tap-changer in converter transformer based on time–frequency vibration analysis," *IEEE Trans. Ind. Electron.*, vol. 63, no. 6, pp. 3815–3823, Jun. 2016.

[21] T. Wang, Y. He, Q. Luo, F. Deng, and C. Zhang, "Self-powered RFID sensor tag for fault diagnosis and prognosis of transformer winding," *IEEE Sensors J.*, vol. 17, no. 19, pp. 6418–6430, Oct. 2017.

[22] T. Wang, Y. He, B. Li, and T. Shi, "Transformer fault diagnosis using self-powered RFID sensor and deep learning approach," *IEEE Sensors J.*, vol. 18, no. 15, pp. 6399–6411, Aug. 2018.

[23] T. Wang, "Fault diagnosis of transformer based on self-powered RFID sensor tag and improved HHT," *J. Elect. Eng. Technol.*, vol. 13, no. 5, pp. 2134–2143, 2018.
[24] J. Guo, Z. Shi, H. Li, D. Zhen, F. Gu, and A. D. Ball, "Early fault diagnosis for planetary gearbox based wavelet packet energy and modulation signal bispectrum analysis," *Sensors*, vol. 18, no. 9, p. 2908, 2018.
[25] S. Osman and W. Wang, "A morphological Hilbert–Huang transform technique for bearing fault detection," *IEEE Trans. Instrum. Meas.*, vol. 65, no. 11, pp. 2646–2656, Nov. 2016.
[26] G. Georgoulas, I. P. Tsoumas, J. A. Antonino-Daviu, V. Climente-Alarcón, C. D. Stylios, E. D. Mitronikas, and A. N. Safacas, "Automatic pattern identification based on the complex empirical mode decomposition of the startup current for the diagnosis of rotor asymmetries in asynchronous machines," *IEEE Trans. Ind. Electron.*, vol. 61, no. 9, pp. 4937–4946, Sep. 2014.
[27] J. Wang and Q. He, "Wavelet packet envelope manifold for fault diagnosis of rolling element bearings," *IEEE Trans. Instrum. Meas.*, vol. 65, no. 11, pp. 2515–2526, Nov. 2016.
[28] Q. B. He, H. Y. Song, and X. X. Ding, "Sparse signal reconstruction based on time-frequency manifold for rolling element bearing fault signature enhancement," *IEEE Trans. Instrum. Meas.*, vol. 65, no. 2, pp. 482–491, Feb. 2016.
[29] L. Ren, W. Lv, S. Jiang, and Y. Xiao, "Fault diagnosis using a joint model based on sparse representation and SVM," *IEEE Trans. Instrum. Meas.*, vol. 65, no. 10, pp. 2313–2320, Oct. 2016.
[30] Z. Du, X. Chen, H. Zhang, and R. Yan, "Sparse feature identification based on union of redundant dictionary for wind turbine gearbox fault diagnosis," *IEEE Trans. Ind. Electron.*, vol. 62, no. 10, pp. 6594–6605, Oct. 2015.
[31] Y. Wang, X. Wang, and W. Liu, "Unsupervised local deep feature for image recognition," *Inf. Sci.*, vol. 351, pp. 67–75, Sep. 2016.
[32] S. Zhan, Q.-Q. Tao, and X.-H. Li, "Face detection using representation learning," *Neurocomputing*, vol. 187, pp. 19–26, Sep. 2016.
[33] N. Marir, H. Wang, G. Feng, B. Li, and M. Jia, "Distributed abnormal behavior detection approach based on deep belief network and ensemble SVM using spark," *IEEE Access*, vol. 6, pp. 59657–59671, 2018.
[34] F. Wu, Z. Wang, W. Lu, X. Li, Y. Yang, J. Luo, and Y. Zhuang, "Regularized deep belief network for image attribute detection," *IEEE Trans. Circuits Syst. Video Technol.*, vol. 27, no. 7, pp. 1464–1477, Jul. 2017.
[35] M. Ahmad, D. Ai, G. Xie, S. F. Qadri, H. Song, Y. Huang, Y. Wang, and J. Yang, "Deep belief network modeling for automatic liver segmentation," *IEEE Access*, vol. 7, pp. 20585–20595, 2019.
[36] M. Xia, T. Li, L. Liu, L. Xu, and C. W. de Silva, "Intelligent fault diagnosis approach with unsupervised feature learning by stacked denoising autoencoder," *IET Sci. Meas. Technol.*, vol. 11, no. 6, pp. 687–695, Sep. 2017.
[37] G. Jiang, H. He, P. Xie, and Y. Tang, "Stacked multilevel-denoising autoencoders: A new representation learning approach for wind turbine gearbox fault diagnosis," *IEEE Trans. Instrum. Meas.*, vol. 66, no. 9, pp. 2391–2402, Sep. 2017.
[38] C. Zhang, Y. Xie, D. Liu, and L. Wang, "Fast threshold image segmentation based on 2D fuzzy Fisher and random local optimized QPSO," *IEEE Trans. Image Process.*, vol. 26, no. 3, pp. 1355–1362, Mar. 2017.

TAO WANG received the B.S. degree in electrical engineering from the Hefei University of Technology, Hefei, China, in 2014, where he is currently pursuing the Ph.D. degree. His current research interests include the research of intelligent and real-time information processing, smart electronics devices, and the diagnosis and prognosis of high voltage equipment.

YIGANG HE (M'17) received the M.Sc. degree in electrical engineering from Hunan University, Changsha, China, in 1992, and the Ph.D. degree in electrical engineering from Xi'an Jiaotong University, Xi'an, China, in 1996.

In 1990, he joined the College of Electrical and Information Engineering, Hunan University, where he was an Associate Professor and a Professor, in 1996 and 1999, respectively. From 2006 to 2011, he was the Director of the Institute of Testing Technology for Circuits and Systems, Hunan University. He was a Senior Visiting Scholar with the University of Hertfordshire, Hatfield, U.K., in 2002. From 2011 to 2017, he was the Head of the School of Electrical Engineering and Automation, Hefei University of Technology. In 2017, he joined Wuhan University, China, where he is currently the Vice Head of the School of Electrical Engineering and Automation. His research interests include power electronic circuit theory and its applications, testing and fault diagnosis of analog and mixed-signal circuits, electrical signal detection, smart grid, satellite communication monitoring, and intelligent signal processing. On the above research areas, he has presided more than a number of state-level projects research such as the National Natural Science Foundation of China, the State Key Program of National Natural Science Foundation of China, the National Key Research and Development Plan "Important Scientific Instruments and Equipment Development," the National High Technology Research and Development Program of China, and the Major State Basic Research Development Program of China. He has published some 300 journals and conference papers which was included more than 1000 times in Science Citation Index of American Institute for Scientific Information in the aforementioned areas and several chapters in edited books.

TIANCHENG SHI was born in 1990. He received the bachelor's degree in engineering from the Hefei University of Technology, in 2013, where he is currently pursuing the Ph.D. degree. His current research interests include fault diagnosis and fault tolerance for power electronics converter systems.

BING LI received the B.E. degree in automobile engineering from Chongqing Science and Technology University, Chongqing, China, in 1995, and the M.E. and Ph.D. degrees in electrical engineering from Hunan University, Changsha, China, in 2006 and 2011, respectively. He has been a Postdoctoral Researcher and a Visiting Scholar with the College of Electrical and Information Engineering, Hunan University, since 2011. He has also been an Associate Professor with the School of Electrical and Automation Engineering, Hefei University, Hefei, China, since 2013. His current research interests include radio-frequency identification technology, wireless sensor networks, and signal processing.